Single-Molecule Magnets Hot Paper

DOI: 10.1002/anie.201407799

A Heterometallic Fe^{II}–Dy^{III} Single-Molecule Magnet with a Record Anisotropy Barrier**

Jun-Liang Liu, Jie-Yi Wu, Yan-Cong Chen, Valeriu Mereacre, Annie K. Powell, Liviu Ungur,* Liviu F. Chibotaru, Xiao-Ming Chen, and Ming-Liang Tong**

Abstract: *A record anisotropy barrier (319 cm^{-1}) for all d-f complexes was observed for a unique Fe^{II}-Dy^{III}-Fe^{II} single-molecule magnet (SMM), which possesses two asymmetric and distorted Fe^{II} ions and one quasi-D_{5h} Dy^{III} ion. The frozen magnetization of the Dy^{III} ion leads to the decreased Fe^{II} relaxation rates evident in the Mössbauer spectrum. Ab initio calculations suggest that tunneling is interrupted effectively thanks to the exchange doublets.*

Single-molecule magnets (SMMs) are well-known molecular materials with the potential for high-density information storage and quantum processing. The characteristic blocking of the magnetization of SMMs arises through the trapping of the magnetic moment in one of the bistable quantum states which are designated by opposite directions of the total magnetic moment.[1,2] In the absence of external perturbations or fields, the SMMs can preserve their magnetic state for a long time. The requirement for this is the suppression of quantum tunneling of magnetization (QTM) in the ground state and a relatively high energy of the excited states through which such reversal of magnetization can occur when one of the lowest excited-state QTM cannot be suppressed. In such cases, the energy barrier to spin reversal effectively defines the temperature range over which the magnetization of a SMM is blocked.

In the case of mononuclear complexes based on lanthanide ions with strong spin–orbit coupling effects, the origin of the blocking barrier is related to the (axial) crystal-field splitting of the ground-state multiplet *J*.[1a,3,4] The axial components of the crystal field stabilize an axial doublet ($g_{x,y}/g_z = 0$, or $\Delta_{tun} = 0$) in the ground state, while the excited spin–orbit states lie much higher in energy.[5]

In polynuclear complexes the situation is more complex, due to magnetic (exchange and dipolar) interactions between various metal sites. Whereas in the low-temperature region (within the exchange spectrum) the exchange interaction increases the magnetization-blocking properties,[6a,7a] in the mid- and high-temperature region (above the exchange spectrum) the presence of neighboring magnetic spins is the source of the fluctuating magnetic field, which enhances the magnetic relaxation.[7b] As a result of these competing factors, it is a challenge to obtain polynuclear SMMs based on 3d and 4f metals possessing high blocking barriers.[6]

Inspired by the magnetic behavior of the single-ion magnet with D_{5h} symmetry, $[Zn^{II}_2Dy^{III}]$ (**1**),[8] we thought it logical to replace the Zn^{II} ion with a paramagnetic divalent 3d ion and thus we prepared the Fe^{II} analogue using Schlenk techniques. Here we report the ferromagnetically coupled coordination complex $[Fe_2Dy(L)_2(H_2O)]ClO_4{\cdot}2H_2O$ [**2**; L = 2,2′,2″-(((nitrilotris(ethane-2,1-diyl))tris(azanediyl))tris(methylene))tris(4-chlorophenol)], which we will refer to as $[Fe^{II}_2Dy^{III}]$. This molecule exhibits a record anisotropy barrier for 3d-4f SMMs of 319 cm^{-1} (459 K). In terms of 3d-*n*f SMMs this is more than three times greater than the next highest barrier of 98.6 cm^{-1} (142 K) found for $[U^{V}_{12}Mn^{II}_6]$.[9a] For comparison, the highest energy barrier for a pure d-SMM system is 226 cm^{-1} for $[Fe^{I}(C(SiMe_3)_3)_2]^-$;[9b] for a pure f-SMM system the highest energy barrier is 652 cm^{-1} for $[Tb^{III}(Pc)(Pc')]$.[9c] Furthermore, $[Fe^{II}_2Dy^{III}]$ is also the first reported Fe^{II}-Dy^{III} SMM.

[*] J.-L. Liu,[+] J.-Y. Wu,[+] Y.-C. Chen, Prof. Dr. X.-M. Chen, Prof. Dr. M.-L. Tong
Key Laboratory of Bioinorganic and Synthetic Chemistry of the Ministry of Education, State Key Laboratory of Optoelectronic Materials and Technologies
School of Chemistry and Chemical Engineering
Sun Yat-Sen University, Guangzhou 510275 (P. R. China)
E-mail: tongml@mail.sysu.edu.cn
Homepage: http://ce.sysu.edu.cn/bisc/members/200809/6440.html

Dr. V. Mereacre, Prof. Dr. A. K. Powell
Institut für Anorganische Chemie
Karlsruhe Institute of Technology (KIT)
Engesserstrasse 15, 76131 Karlsruhe (Germany)
E-mail: annie.powell@kit.edu

Prof. Dr. A. K. Powell
Institute of Nanotechnology (INT)
Karlsruhe Institute of Technology (KIT)
P.O. Box 3640, 76021 Karlsruhe (Germany)

Dr. L. Ungur, Prof. Dr. L. F. Chibotaru
Theory of Nanomaterials Group and
INPAC—Institute of Nanoscale Physics and Chemistry
Katholieke Universiteit Leuven
Celestijnenlaan 200F, 3001 Leuven (Belgium)
E-mail: Liviu.Ungur@chem.kuleuven.be

[+] These authors contributed equally to this work.

[**] This work was supported by the "973 Project" (2012CB821704 and 2014CB845602), the NSFC (grant nos. 91122032, 21121061, and 21371183), the NSF of Guangdong (S2013020013002), and the DFG transregional collaborative research center SFB/TRR 88 "3MET". L.U. is a postdoctoral fellow of the Fonds Wetenschappelijk Onderzoek-Vlaanderen and also gratefully acknowledges INPAC and Methusalem grants from KU Leuven.

Supporting information for this article is available on the WWW under http://dx.doi.org/10.1002/anie.201407799.

 © 2014 Wiley-VCH Verlag GmbH & Co. KGaA, Weinheim

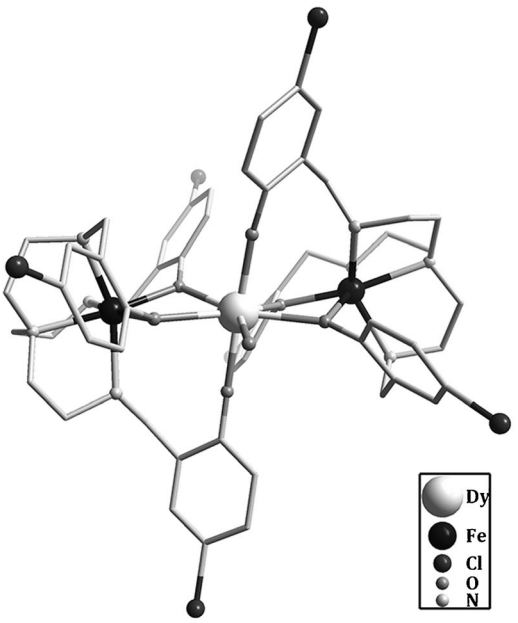

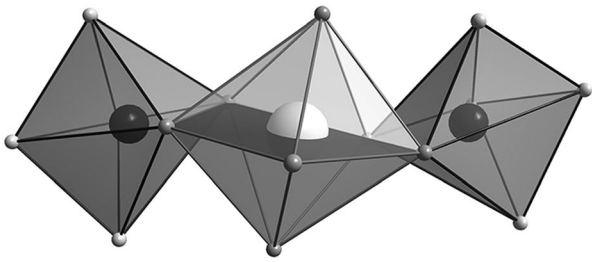

Figure 1. Structural motifs of the [Fe^{II}-Dy^{III}-Fe^{II}] cores of [$Fe^{II}_2Dy^{III}$]. Hydrogen atoms have been omitted for clarity.

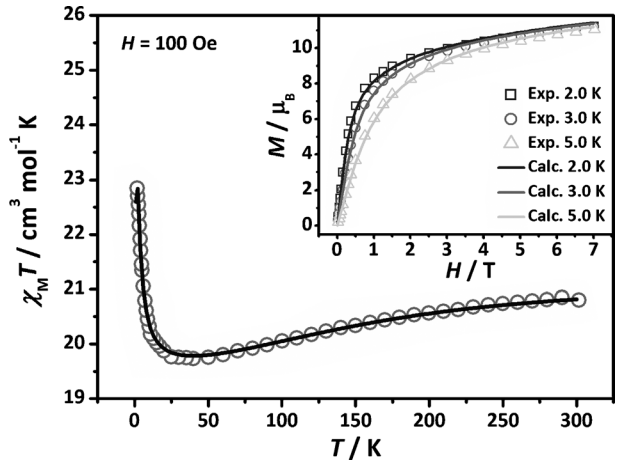

Figure 2. Temperature dependence of the $\chi_M T$ product at 100 Oe for [$Fe^{II}_2Dy^{III}$]. Inset: Plot of *M* versus *H* at 2, 3, and 5 K. The solid lines correspond to ab initio calculations with the fitting parameters. The calculated magnetization curves (in the inset) corresponds to the fitted parameters reported in Table 1.

Although the structure of the [$Fe^{II}_2Dy^{III}$] complex **2** (Figure 1) is similar to that of the [$Zn^{II}_2Dy^{III}$] complex **1**, the synthesis (see the Experimental Section in the Supporting Information) must be performed under anaerobic conditions to prevent oxidation of the Fe^{II}. Each Fe^{II} ion is chelated by one tripodal ligand to give an aza-Fe^{II}-atrane-like structure,[10] and these units are linked to the central Dy^{III} through their phenoxyl groups. The remaining two phenoxy groups axially coordinate along the pseudo-fivefold axis of the central Dy^{III} ion.

There are two significant structural differences between **1** and **2**. Firstly, the terminal methanol ligand on Dy^{III} in [$Zn^{II}_2Dy^{III}$] **1** is replaced by a water molecule in [$Fe^{II}_2Dy^{III}$] **2**. This means that the Dy–O bond length is significantly longer in [$Fe^{II}_2Dy^{III}$] at 2.492(7) Å than in [$Zn^{II}_2Dy^{III}$] where it is 2.427(6) Å, (Table S2.2). This results in the pentagonal-bipyramid (D_{5h}, see the CShM values[11] in Table S2.3) coordination polyhedron of Dy^{III} being more oblate for [$Fe^{II}_2Dy^{III}$]. Secondly, the two Fe^{II} have very different coordination geometries. Fe1 is close to octahedral (O_h) while Fe2 is closer to trigonal prismatic (C_{3v}), although they both deviate from the idealized geometries. Mössbauer spectroscopy confirmed the +2 oxidation state on both Fe^{II} centers and slow paramagnetic relaxation and magnetic hyperfine splitting indicate that the Fe^{II} atoms feel a strong magnetic field owing to the slow magnetization reversal of the Dy^{III} ion.

As shown in Figure 2, the measured $\chi_M T$ value (20.8 $cm^3 K mol^{-1}$) at 300 K is very close to that expected (20.2 $cm^3 K mol^{-1}$; Dy^{III}: 14.2 $cm^3 K mol^{-1}$ for $^6H_{15/2}$, Fe^{II}: 3.00 $cm^3 K mol^{-1}$ for the spin-only case).[12] For the pentagonal-bipyramid Dy^{III} ion, the ground-state spin–orbit-coupled $^6H_{15/2}$ term is split into eight Kramers doublets by the crystal field (ca. 6.4×10^2 cm^{-1}, according to ab initio calculations). For the two Fe^{II} ions, the obvious geometric distortion removes the degeneracy of the octahedral ground-state $^5T_{2g}$ term, leading to partial quenching of the first-order spin–orbit coupling. However, the presence of the second-order spin–orbit interaction leads to relatively strong zero-field splitting (ZFS) of the quintet ground state. These two effects, mainly the former, make the $\chi_M T$ product decrease slightly to 19.7 $cm^3 K mol^{-1}$ at 40 K. On further cooling, the ferromagnetic interaction between Dy^{III}-Fe^{II} leads to a strong increase and $\chi_M T$ reaches 22.9 $cm^3 K mol^{-1}$ at 1.8 K. The ferromagnetically coupled [Fe^{II}-Dy^{III}-Fe^{II}] unit remains a Kramers system, which can guarantee that the ground state is at least doubly degenerate rather than a singlet according to Kramers theorem.[4a,13] This ferromagnetic coupling together with the quasi-D_{5h} symmetry of the Dy^{III} ion are favorable for this system to show SMM behavior.

Significant slow relaxation of magnetization is observed in ac susceptibilities under zero dc field (Figure 3; Figures S3.1 and S3.2). The very high ac peak temperature and strong frequency dependence of the ac susceptibilities both suggest a thermally activated slow magnetic relaxation process. Fitting the relaxation times and temperatures with an Arrhenius equation, we get an anisotropy barrier as large as 319 cm^{-1} (459 K), and $\tau_0 = 1.11 \times 10^{-10}$ s. The α values extracted from the generalized Debye model are in the range 0.07–0.19 (Figure S3.3) suggesting a relatively narrow distribution of the relaxation times.[1a,14]

© 2014 Wiley-VCH Verlag GmbH & Co. KGaA, Weinheim

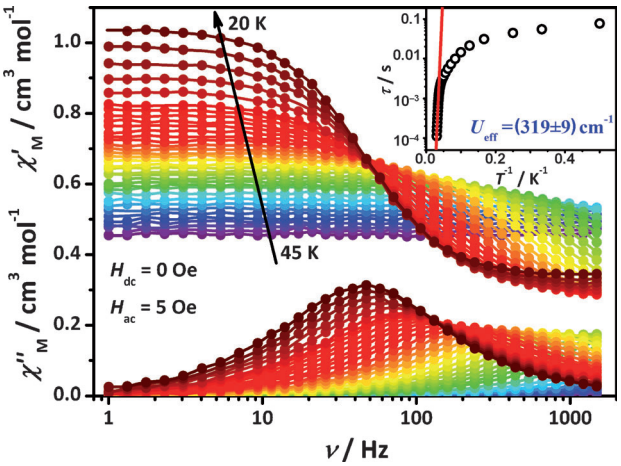

Figure 3. Plot of susceptibility versus frequency in the temperature range of 20–45 K at $H_{dc}=0$ Oe ($H_{ac}=5$ Oe) for [$Fe^{II}_2Dy^{III}$]. Inset: Plot of the relaxation time τ (logarithmic scale) versus T^{-1} obtained from $\chi_M''(\nu)$. The solid lines correspond to an Arrhenius law.

Ab initio calculations of the CASSCF/RASSI/SINGLE ANISO type of the individual metal sites (see the Supporting Information for computational details and most of the results) revealed the very strong axiality of the ground-state Kramers doublet of the Dy^{III} site, and a large energy separation between the ground-state and first-excited-state Kramers doublets. This is in agreement with the strong anisotropy obtained for Dy^{III} in quasi-D_{5h} symmetry in [$Zn^{II}_2Dy^{III}$].[8] The spectrum of the eight lowest Kramers doublets originating from the ground-state atomic multiplet $J={}^{15}/_{2}$ is shown in Table S5.3. Calculations reveal the relatively strong zero-field splitting on both Fe^{II} centers (five low-lowest levels in Table S5.6). The results obtained by ab initio calculations for individual metal centers were employed to compute the exchange spectrum and magnetic properties of the trinuclear complex using the POLY_ANISO program.[6b,15] The magnetic interactions between Dy^{III} and Fe^{II} sites were considered within the Lines model (see the Supporting Information for more details), while the contribution of the dipole–dipole magnetic coupling is accounted exactly. The exchange coupling parameters have been estimated by BS-DFT calculations employed within the ORCA 3.0.0 program[7] (see the Supporting Information for more details). Their values are given in Table 1 together with best-fitted Lines parameters. Finally, the magnetic properties have been computed on the basis of the obtained exchange spectrum (Figure 2).

The extracted blocking barrier from the ac measurements (319 cm^{-1}, Figure 3) is in good agreement with the energy of the first excited Kramers doublet of Dy^{III} obtained in ab initio calculations (313.9 cm^{-1}, Table S5.9). The possible reasons why this complex has such a large blocking barrier are: 1) the non-axial parameters of the crystal field are very small in a quasi-D_{5h} local symmetry, leading to high Ising-type anisotropy;[5,8] 2) the energy of the first excited Kramers doublet of the Dy^{III} ion in **2** is larger (313.9 cm^{-1}) than that in **1** (289.9 cm^{-1}). This enhancement may originate from the more axial geometry (see above) of Dy^{III} in **2**, in particular, shorter Dy–O bonds for axial ligands. The premise that the corresponding oxygen atoms make the main contribution to the axial anisotropy on Dy(III) is confirmed by the fact that the anisotropy axis passes almost exactly through these atoms (Figure 4).

Table 1: Exchange coupling parameters employed within the Lines model for the computation of the electronic spectrum, and magnetism of **2** (in cm^{-1}).

	BS-DFT[7]	Fitting
Fe1–Dy	0.84	0.38
Fe2–Dy	0.50	0.06
Fe1–Fe2	−0.20	0.09

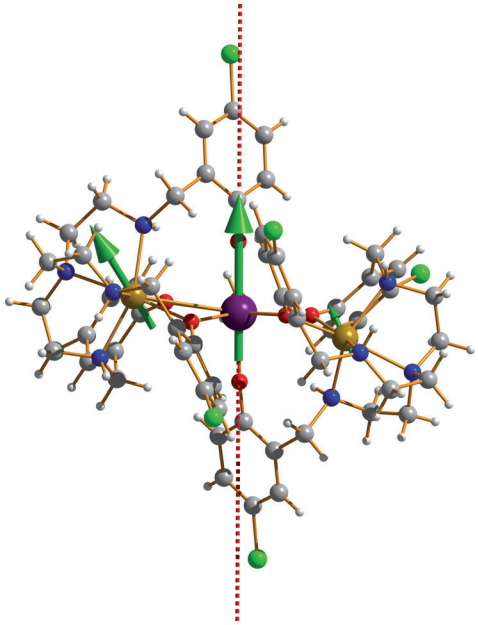

Figure 4. Orientations of the main magnetic moments on metal sites in the ground exchange state of the investigated [$Fe^{II}_2Dy^{III}$]; gray C, white H, green Cl, violet Dy, yellow Fe, blue N, red O. Magnetic moments on Fe sites in the ground state of the molecule form significant angles with the main anisotropy axis of Dy (32.6° for Fe1 and 33.4° for Fe2) owing to relatively strong local anisotropy on the iron sites. Note the much smaller magnetic moment on the Fe2 site.

The analysis of the wave function of the low-lying exchange Kramers doublets shows that the contribution of the magnetic moment of Fe2 (D_{3h} geometry) is very small (Figure 4). This is explained by a relatively large ZFS splitting of the lowest doublet on Fe2 (Table S5.6) compared to Fe2–Dy exchange interaction. In contrast, the exchange interaction in Fe1–Dy is much larger (Table 1) while the ZFS on Fe1 (O_h geometry) is comparable to that of Fe2. As a result, the magnetism of the low-lying exchange states (Table S5.9) basically corresponds to a Fe1–Dy exchange-coupled dimer, while the effectively uncoupled Fe2 site is largely non-magnetic. Nevertheless the low-lying exchange Kramers doublets appear to be strongly axial ($g_{x,y}<10^{-5}$), implying a suppressed QTM which is ultimately due to the strong axiality of the Dy^{III} site (Table S5.3).

© 2014 Wiley-VCH Verlag GmbH & Co. KGaA, Weinheim

Although slow relaxation effects were detected for a series of high-spin Fe^{II} compounds,[16] the ^{57}Fe Mössbauer spectra of high-spin Fe^{II} compounds generally reveal fast spin relaxation even at liquid-helium temperatures and quadrupole-split doublets are observed. This is because in Fe^{II} systems spin–lattice relaxation[17] is an important relaxation mechanism and expected to be very fast due to the non-S-state character of the Fe^{II} ion.[18] The Mössbauer spectrum of $[Fe^{II}_2Y^{III}]$ (**3**, the analogue of $[Fe^{II}_2Dy^{III}]$) at 3 K (Figure S4.1) consists of a doublet, indicative of fast magnetic relaxation. The values of isomer shift, $\delta = 1.15\ mm\,s^{-1}$, and quadrupole interaction, $\Delta E_Q = 3.37\ mm\,s^{-1}$, are in line with what can be expected for the average value for Fe^{II} ions in distorted octahedral ligand fields. In contrast to $[Fe^{II}_2Y^{III}]$, the Mössbauer spectrum of $[Fe^{II}_2Dy^{III}]$ at 3 K (Figure S4.2) represents a very complex magnetic spectrum arising from the overlap of two magnetic patterns. Two patterns are required because the different moments for the two distinct Fe^{II} coordination environments are no longer averaged. The observation of these sextets demonstrates that the magnetic relaxation is much slower than that observed in $[Fe^{II}_2Y^{III}]$. Taking into account that these two compounds are isostructural, the slowing down of the magnetic relaxation of the Fe^{II} moments must arise from interactions with the central anisotropic, magnetically aligned Dy^{III} ion. Such an effect has been observed for several Fe^{III}-Dy^{III}-containing molecular clusters,[19a,b] but rarely in Fe^{II}-Dy^{III}-containing clusters.[19c] Given that the exchange interaction between Dy^{III} and Fe^{II} ions is relatively small, the observed interaction is probably dominated by magnetic dipolar effects.

The spin–spin and spin–lattice relaxation rates in the presence of the anisotropic Dy^{III} ion, which mediates the interaction between two Fe^{II} ions in $[Fe^{II}_2Dy^{III}]$, are expected to decrease ($< 10^{-7}$ s), due to the significant decrease in the distance between the spin systems and the increased number of available spin states compared with the Y^{III} analogue. Since the Mössbauer spectrum clearly shows the opposite trend, this must be connected to the influence of the ionic anisotropy of the Dy^{III} ions. These observations can be understood in terms of slow intracluster relaxation and an internal dipolar field resulting from the nonreversal of the magnetization of the Dy^{III} ions at low temperature. This implies that the magnetic field experienced by the Fe^{II} cations in the vicinity of magnetic Dy^{III} ions can be viewed as static on the Mössbauer timescale. Such behavior is expected because the Mössbauer timescale is on the order of magnitude of 10^{-7} s while the Dy^{III} ion magnetization reversal time in $[Fe^{II}_2Dy^{III}]$ several orders of magnitude larger at low temperatures making the presence of the Dy^{III} ion in the compound is seen as crucial to the spin structure. In addition, preliminary simulations show different hyperfine fields on iron nuclei. This is in line with the results of the ab initio calculations which suggest it should be possible to differentiate between the Fe^{II} ion in the Fe1–Dy exchange-coupled dimer and the effectively uncoupled Fe2 site.

A further peculiarity of this system is observed in the Mössbauer spectra under applied magnetic field. When an external magnetic field is applied, the Mössbauer spectra for $[Fe^{II}_2Dy^{III}]$ exhibit patterns[20] and hyperfine parameters similar to those observed in $[Fe^{II}_2Y^{III}]$ (Figure S4.2). This suggests that the anisotropy responsible for the magnetic spectrum of $[Fe^{II}_2Dy^{III}]$ at 3 K in zero field has been somehow quenched. Similar effects were recently reported for a series of Fe^{III}-Dy^{III} compounds.[19b] The probable cause of this quenching is that under application of a strong external static magnetic field, the relaxation of the magnetization of the Dy^{III} ions becomes faster and the average moment and internal molecular magnetic field tend towards zero. As a result, the Fe nuclei no longer sense the magnetic field from the fast relaxing Dy^{III} neighbors that look like "unpinned". This is further complicated by the very strong spin–orbit contributions from the high-spin Fe^{II} ions. The fact that in this system the two Fe^{II} ions have different levels of distortion from the idealized octahedral coordination sphere adds a further level of complexity to the situation.

The interpretation of the Mössbauer results presented can be regarded as a qualitative discussion of the cause of the observed behavior. Nevertheless, the results are consistent with those of the ab initio calculations and it will be the goal of future work to compare results from methods such as EPR spectroscopy, magnetocircular dichroism, and inelastic neutron scattering and, if possible, single-crystal studies.

To summarize, we have synthesized a unique Fe^{II}-Dy^{III}-Fe^{II} single-molecule magnet with a pentagonal-bipyramid (D_{5h}) Dy^{III} ion, and two asymmetric and distorted Fe^{II} ions. Ab initio calculations suggest that the height of the barrier corresponds to the energy of the first excited Kramers doublet on the Dy^{III} site. The increased blocking barrier in **2** compared to **1** reflects the enhancement of the axial crystal field in the former compound, which arises through modifications of the geometry of the nearest environment of Dy^{III} when diamagnetic zinc ions are replaced by paramagnetic iron ions. This leads to a record anisotropy barrier for 3d-4f SMMs, and, indeed, all d-f SMMs of $319\ cm^{-1}$ (459 K). The frozen magnetic moment of the Dy^{III} ion at low temperatures is responsible for slowing down the magnetic relaxation of Fe^{II} moments which is observed in the Mössbauer spectrum at zero applied field.

Received: July 31, 2014
Published online: September 24, 2014

Keywords: ab initio calculations · anisotropy barriers · ferromagnetic interactions · magnetic properties · Mössbauer spectroscopy · single-molecule magnet

[1] a) D. Gatteschi, R. Sessoli, J. Villain, *Molecular Nanomagnets*, Oxford University Press, New York, **2006**; b) A. Dei, D. Gatteschi, *Angew. Chem. Int. Ed.* **2011**, *50*, 11852 – 11858; *Angew. Chem.* **2011**, *123*, 12054 – 12060; c) D. Gatteschi, R. Sessoli, *Angew. Chem. Int. Ed.* **2003**, *42*, 268 – 297; *Angew. Chem.* **2003**, *115*, 278 – 309; d) M. N. Leuenberger, D. Loss, *Nature* **2001**, *410*, 789 – 793; e) W. Wernsdorfer, R. Sessoli, *Science* **1999**, *284*, 133 – 135.

[2] a) R. Sessoli, D. Gatteschi, A. Caneschi, M. A. Novak, *Nature* **1993**, *365*, 141 – 143; b) R. Sessoli, H. L. Tsai, A. R. Schake, S. Wang, J. B. Vincent, K. Folting, D. Gatteschi, G. Christou, D. N. Hendrickson, *J. Am. Chem. Soc.* **1993**, *115*, 1804 – 1816.

[3] N. Ishikawa, M. Sugita, T. Ishikawa, S.-y. Koshihara, Y. Kaizu, *J. Am. Chem. Soc.* **2003**, *125*, 8694 – 8695.

 © 2014 Wiley-VCH Verlag GmbH & Co. KGaA, Weinheim

[4] a) J. D. Rinehart, J. R. Long, *Chem. Sci.* **2011**, *2*, 2078 – 2085; b) L. Sorace, C. Benelli, D. Gatteschi, *Chem. Soc. Rev.* **2011**, *40*, 3092 – 3105; c) R. Sessoli, A. K. Powell, *Coord. Chem. Rev.* **2009**, *253*, 2328 – 2341.

[5] L. Ungur, L. F. Chibotaru, *Phys. Chem. Chem. Phys.* **2011**, *13*, 20086 – 20090.

[6] a) K. C. Mondal, A. Sundt, Y. Lan, G. E. Kostakis, O. Waldmann, L. Ungur, L. F. Chibotaru, C. E. Anson, A. K. Powell, *Angew. Chem. Int. Ed.* **2012**, *51*, 7550 – 7554; *Angew. Chem.* **2012**, *124*, 7668 – 7672; b) L. Ungur, M. Thewissen, J.-P. Costes, W. Wernsdorfer, L. F. Chibotaru, *Inorg. Chem.* **2013**, *52*, 6328 – 6337; c) J.-L. Liu, F.-S. Guo, Z.-S. Meng, Y.-Z. Zheng, J.-D. Leng, M.-L. Tong, L. Ungur, L. F. Chibotaru, K. J. Heroux, D. N. Hendrickson, *Chem. Sci.* **2011**, *2*, 1268 – 1272; d) J.-D. Leng, J.-L. Liu, M.-L. Tong, *Chem. Commun.* **2012**, *48*, 5286 – 5288; e) J.-L. Liu, Y.-C. Chen, Q.-W. Li, S. Gómez-Coca, D. Aravena, E. Ruiz, J.-D. Leng, M.-L. Tong, *Chem. Eur. J.* **2013**, *19*, 17567 – 17577; f) J.-L. Liu, Y.-C. Chen, Q.-W. Li, S. Gómez-Coca, D. Aravena, E. Ruiz, W.-Q. Lin, J.-D. Leng, M.-L. Tong, *Chem. Commun.* **2013**, *49*, 6549 – 6551; g) J.-L. Liu, W.-Q. Lin, J.-D. Leng, Y.-C. Chen, F.-S. Guo, M.-L. Tong, *Inorg. Chem.* **2013**, *52*, 457 – 463.

[7] a) "The ORCA program system": F. Neese, *Wiley Interdiscip. Rev. Comput. Mol. Sci.* **2012**, *2*, 73 – 78; b) T. Soda, Y. Kitagawa, T. Onishi, Y. Takano, Y. Shigeta, H. Nagao, Y. Yoshioka, K. Yamaguchi, *Chem. Phys. Lett.* **2000**, *319*, 223 – 230; c) S. K. Langley, D. P. Wielechowski, V. Vieru, N. F. Chilton, B. Moubaraki, L. F. Chibotaru, K. S. Murray, *Chem. Sci.* **2014**, *5*, 3246 – 3256.

[8] J.-L. Liu, Y.-C. Chen, Y.-Z. Zheng, W.-Q. Lin, L. Ungur, W. Wernsdorfer, L. F. Chibotaru, M.-L. Tong, *Chem. Sci.* **2013**, *4*, 3310 – 3316.

[9] a) V. Mougel, L. Chatelain, J. Pécaut, R. Caciuffo, E. Colineau, J.-C. Griveau, M. Mazzanti, *Nat. Chem.* **2012**, *4*, 1011 – 1017; b) J. M. Zadrozny, D. Xiao, M. Atanasov, G. J. Long, F. Grandjean, F. Neese, J. R. Long, *Nat. Chem.* **2013**, *5*, 577 – 581; c) C. R. Ganivet, B. Ballesteros, G. de La Torre, J. M. Clemente-Juan, E. Coronado, T. Torres, *Chem. Eur. J.* **2013**, *19*, 1457 – 1465.

[10] J. G. Verkade, *Coord. Chem. Rev.* **1994**, *137*, 233 – 295.

[11] a) S. Alvarez, P. Alemany, D. Casanova, J. Cirera, M. Llunell, D. Avnir, *Coord. Chem. Rev.* **2005**, *249*, 1693 – 1708; b) D. Casanova, P. Alemany, J. M. Bofill, S. Alvarez, *Chem. Eur. J.* **2003**, *9*, 1281 – 1295; c) S. Alvarez, D. Avnir, M. Llunell, M. Pinsky, *New J. Chem.* **2002**, *26*, 996 – 1009.

[12] a) R. L. Carlin, *Magnetochemistry*, Springer-Verlag, Berlin, **1986**; b) O. Kahn, *Molecular Magnetism*, VCH, New York, **1993**.

[13] H. A. Kramers, *Proc. Amsterdam Acad.* **1930**, *33*, 959 – 972.

[14] K. S. Cole, R. H. Cole, *J. Chem. Phys.* **1941**, *9*, 341 – 351.

[15] a) Y.-N. Guo, G.-F. Xu, W. Wernsdorfer, L. Ungur, Y. Guo, J. Tang, H.-J. Zhang, L. F. Chibotaru, A. K. Powell, *J. Am. Chem. Soc.* **2011**, *133*, 11948 – 11951; b) A. Bhunia, M. T. Gamer, L. Ungur, L. F. Chibotaru, A. K. Powell, Y. Lan, P. W. Roesky, F. Menges, C. Riehn, G. Niedner-Schatteburg, *Inorg. Chem.* **2012**, *51*, 9589 – 9597.

[16] a) C. Nicolini, W. M. Reiff, *Inorg. Chem.* **1980**, *19*, 2676 – 2679; b) M. A. Martinez Lorente, F. Dahan, V. Petrouleas, A. Bousseksou, J.-P. Tuchagues, *Inorg. Chem.* **1995**, *34*, 5346 – 5357; c) W. M. Reiff, A. M. LePointe, E. H. Witten, *J. Am. Chem. Soc.* **2004**, *126*, 10206 – 10207.

[17] D. C. Price, C. E. Johnson, I. Marteense, *J. Phys. C* **1977**, *10*, 4843 – 4854.

[18] K. W. H. Stevens, *Rep. Prog. Phys.* **1967**, *30*, 189 – 226.

[19] a) V. Mereacre, F. Klöwer, Y. Lan, R. Clérac, J. A. Wolny, V. Schünemann, C. E. Anson, A. K. Powell, *Beilstein J. Nanotechnol.* **2013**, *4*, 807 – 814; b) A. Baniodeh, V. Mereacre, N. Magnani, Y. Lan, J. A. Wolny, V. Schünemann, C. E. Anson, A. K. Powell, *Chem. Commun.* **2013**, *49*, 9666 – 9668; c) T. Yamaguchi, J.-P. Costes, Y. Kishima, M. Kojima, Y. Sunatsuki, N. Brefuel, J.-P. Tuchagues, L. Vendier, W. Wernsdorfer, *Inorg. Chem.* **2010**, *49*, 9125 – 9135.

[20] We have done a preliminary fit without constraining D, E/D, g, β (angle between the magnetic anisotropy axis and the electric field gradient axis) and observed similar hyperfine parameters for both compounds. The exact analysis of the A matrix requires additional analysis.

 © 2014 Wiley-VCH Verlag GmbH & Co. KGaA, Weinheim